

MICROBANDS IN 80% DRAWN COPPER SINGLE CRYSTALS WITH  
<111> AND <100> STARTING ORIENTATIONS

S. HORIUCHI

*National Institute for Researches in Inorganic  
Materials, Sakura-mura, Niihari-gun, Ibaraki,  
300-31 Japan*

K. ASAKURA

*Department of Metallurgy, Faculty of Engineering,  
University of Tokyo, Bunkyo-ku, Tokyo, 113 Japan*

G. WASSERMANN and J. GREWEN

*Institut für Metallkunde und Metallphysik der TU  
Clausthal, 3398 Clausthal-Zellerfeld, Grosser  
Bruch 23, FRG*

*(Received February 28, 1975)*

*Abstract:* Copper single crystals with the starting orientations <111> and <100> were drawn 80%. In the core region of the rods the orientations and the microstructures were investigated. The stable <111> crystal had a structure consisting of equiaxed cells and microbands which were formed parallel to the {111} planes with the exception of the {111} plane in the cross section of the rod. The <100> orientation was not entirely stable; the beginning of some orientational changes was observed at a high degree of deformation. In the parts with stable orientation a cylindrical cell structure was found with the long axes parallel to the drawing direction. Single microbands formed locally. Dislocation tangles around them finally developed, which lead to a change of the <100> orientation.

## INTRODUCTION

In a previous publication<sup>1</sup> it was shown that copper single crystals with starting orientations near <111>

reached the stable  $\langle 111 \rangle$  orientation during drawing while they homogeneously changed their orientation in the core region of the rod. In a crystal drawn to 95%, this region had triangular outlines in the plane perpendicular to the rod axis, and the triangles were bounded by the intersections of the  $\{111\}$  planes with the cross section. Moreover, linearly arranged lines were observed in a microscope, and it was thought that they could be twin traces although no twin orientation was detected by x-rays.

An electron microscopic investigation<sup>2</sup> revealed that microbands were formed in copper single crystals drawn through a die even at low degrees of deformation. Microbands were first found in rolled silicon iron crystals and they were described as band-like dislocation-free areas with small angle boundaries.<sup>3,4</sup> The density of the microbands in the drawn copper single crystals increased with the degree of deformation and some microbands joined together on drawing to 90%. They lie parallel to the drawing direction. It was assumed that they originated from the elongation of the cells previously formed.<sup>2</sup>

The microscopic picture of the cross section of copper single crystals with starting orientation near  $\langle 100 \rangle$  showed deformation bands in the core region of the rod.<sup>2,5</sup> These deformation bands are areas of uniform orientation first described by Barrett.<sup>6</sup> The  $\langle 100 \rangle$  orientation is not stable at very high degrees of deformation. In the center of these copper rods it was stable up to 90% deformation, while at 99.5% deformation only 50% of the material was in the starting orientation. Cell elongation occurred in the  $\langle 100 \rangle$  crystals in the same manner as in the  $\langle 111 \rangle$  crystals.<sup>2</sup> Moreover, the cells elongated by disappearance of the cell boundaries perpendicular to the long axes of the microbands. It was considered that the microband formation had a direct connection with the reduction of the  $\langle 100 \rangle$  orientation.

## EXPERIMENTS

Copper single crystal rods with a purity of 99.9% were produced by the Bridgman method (12.5 mm diameter, 150 mm length). Two crystals with  $\langle 111 \rangle$  and  $\langle 100 \rangle$  orientations were chemically etched in order to remove the surface layer, and drawn in the length direction to 5.5 mm in diameter at room temperature, i.e. 80% reduction of area. The drawing was done as usual through dies with an angle of  $4^\circ$  in 55 passes at a rate of 4.5 m/min. The sections of the rods were examined by using an optical microscope after etching by either of the following solutions: (1) 10 g  $(\text{NH}_4)_2[\text{CuCl}_4] \cdot 2\text{H}_2\text{O} +$

120 ml H<sub>2</sub>O or (2) 10 g (NH<sub>4</sub>)<sub>2</sub>S<sub>2</sub>O<sub>8</sub> + 100 ml H<sub>2</sub>O. In order to examine the orientation and its spread the core of the rods (1 mm in diameter) was cut out and pole figures were determined for the cross section. Vickers microhardness (load 15 g) was also measured on the cross section.

The microstructures in the core of the rods were examined by means of transmission electron microscopes (100 and 150 kV). Thin discs (1 mm in thickness) were mechanically cut from the rods parallel or perpendicular to the drawing direction. After being thinned chemically to about 0.1 mm thickness, they were electro-polished in a solution of 50 cc HNO<sub>3</sub> + 150 cc CH<sub>3</sub>OH at -20°C.

## RESULTS AND INTERPRETATION

### *The <111> Crystal*

When the <111> single crystal was drawn to 80%, a triangular cross section extending parallel to the rod axis was formed in the core of the rod.<sup>1</sup> The sides of the triangle had a length of about 2.5 mm and the {111} pole figure taken from the core showed that the orientation was <111> with some spread (Figure 1). The hardness number was between 116 and 127.

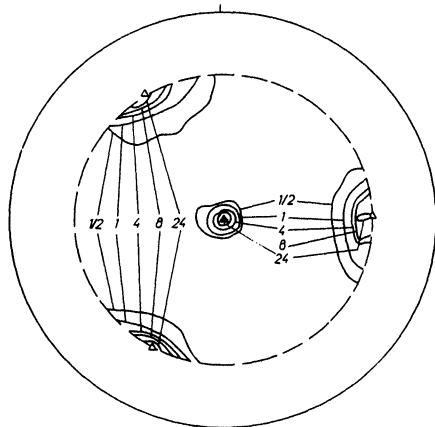


FIGURE 1. {111} pole figure showing the texture formed in the core of the <111> crystal. Plane of projection is the cross section of the rod. Intensities are in arbitrary units. The triangles indicate the ideal <111> orientation.

Figure 2 is an optical micrograph of the cross section. Etch pits were formed and some of them are arranged in lines, running almost parallel to the <110>

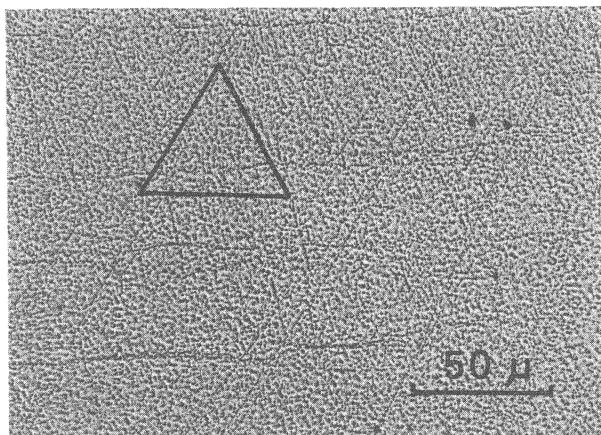


FIGURE 2. Optical micrograph of the core of the  $\langle 111 \rangle$  crystal. The  $\langle 111 \rangle$  drawing direction is perpendicular to the picture and the  $\langle 110 \rangle$  directions in the cross section are indicated. The sample is etched by solution (1).

directions. On the longitudinal sections linearly arrayed etch pits were also observed. An analysis of these etch pit lines indicated that they appeared at the intersection of the  $\{111\}$  planes with the specimen plane and it is assumed that they are identical with the traces previously found.<sup>1</sup>

An electron microscopic observation of the specimen, cut parallel to the cross section (Figure 3a), revealed dislocation cells, having diameters of about 0.5 microns. Among them, microbands were frequently observed. Their boundaries were sharp and the directions in which they extended were well defined. The frequency of the microband formation varied; in most cases a few microbands joined together. Such groups of microbands were dispersed in the plane of the foil with a distance of several or several ten microns. Some of the groups consisted of a large number of microbands. The thickness of most microbands was in the range between 0.1 and 0.2 microns.

An electron diffraction pattern (Figure 3b) taken from the encircled area 1 in Figure 3a shows that the foil plane is parallel to  $(111)$ . The long direction of the microbands is parallel to  $[\bar{1}01]$ . The maximum splitting of the spots is  $10^\circ$  and the number of the microbands within the selected area is about 10. The mean misorientation across a microband boundary is therefore about  $1^\circ$ . Diffraction patterns were also taken from the areas 2 and 3 (Figure 3c and 3d). These reveal the same misorientation across the microband

boundaries, but the lattice rotation occurs in opposite directions in the two areas, i.e. it is anticlockwise in area 2 and clockwise in area 3. As a result, the total misorientation is not very large. In the same foil, microbands extending in the  $[0\bar{1}1]$  or  $[1\bar{1}0]$  directions were observed with almost the same frequency as for the  $[\bar{1}01]$  microband.

Microbands were also found in a foil prepared parallel to the longitudinal section of the rod. Figure 4a shows a typical structure, in which five microbands are joined together in the center. They are longer and their boundaries are sharper than those in Figure 3a. Figure 4b is the diffraction pattern taken from the encircled region in Figure 4a, showing that the foil plane is  $(\bar{1}01)$ . The microbands do not extend parallel to the drawing direction ( $[111]$ ) but almost parallel to the  $[12\bar{1}]$  direction. The splitting of the diffraction spots is about  $10^\circ$ , suggesting that the misorientation across a micro-

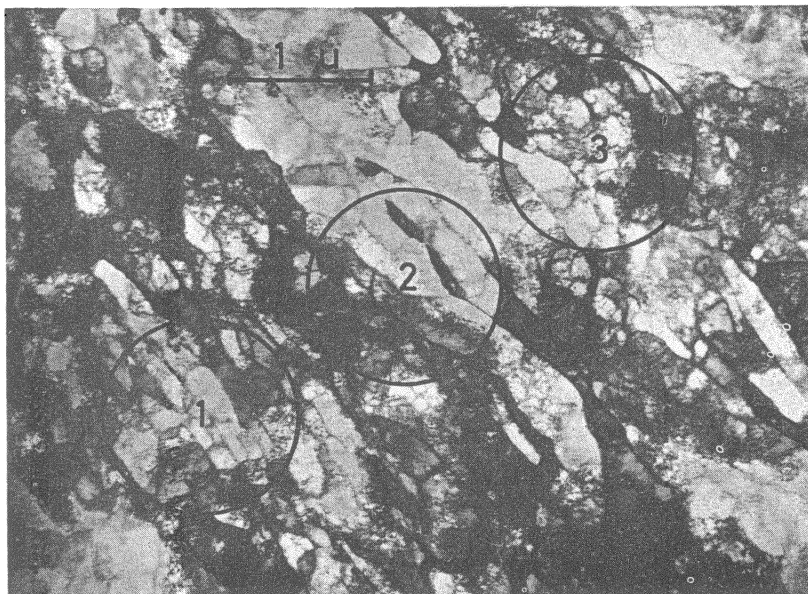
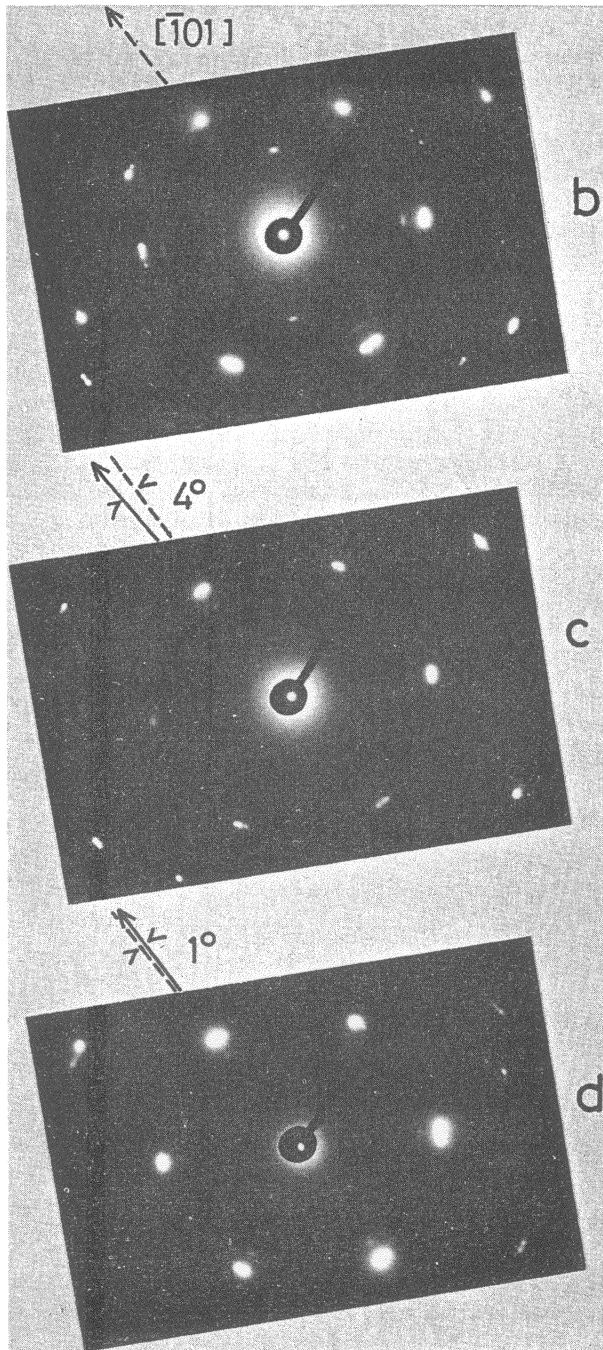
**a**

FIGURE 3a-d. Electron microscopic examination of the  $(11\bar{1})$  plane perpendicular to the  $[111]$  drawing direction (cross section of the rod). (a) Structure with cells and microbands extending in the  $[\bar{1}01]$  direction. Diffraction patterns taken from areas 1 (b), 2 (c) and 3 (d) of Figure 3a. The center directions of the orientation spread in each area are shown by arrows.



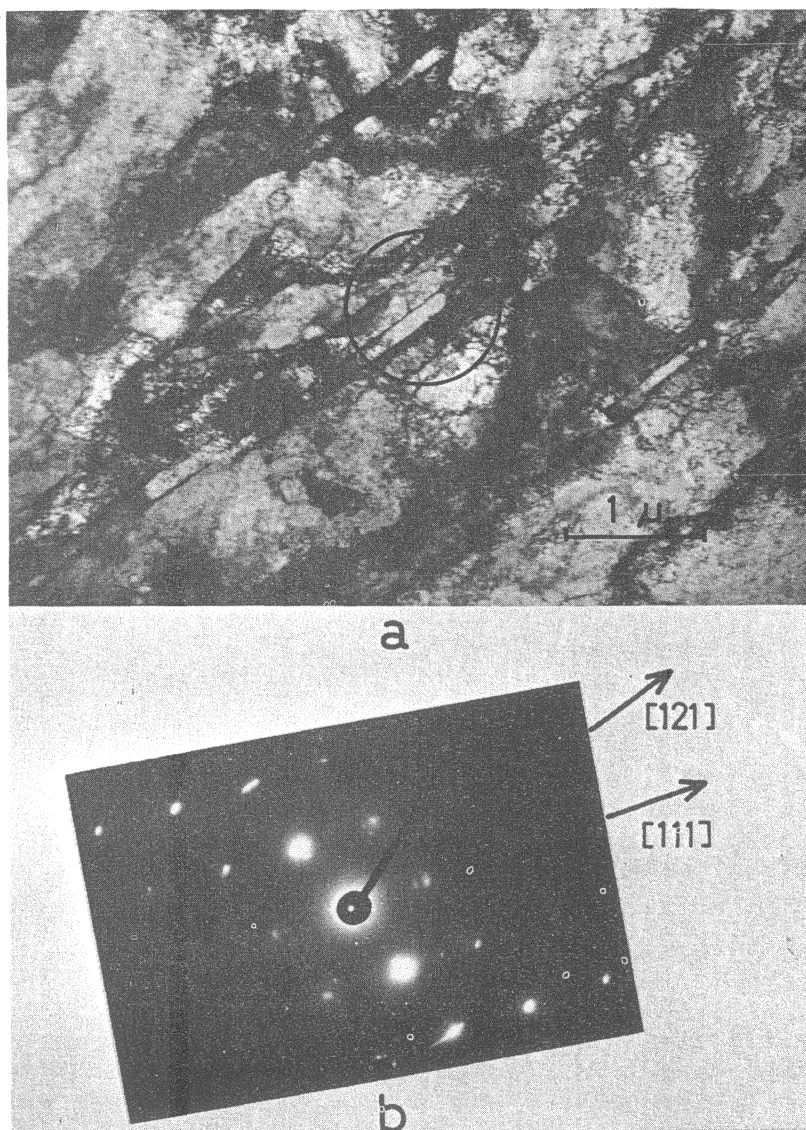


FIGURE 4a and b. Electron microscopic observations of a foil parallel to the  $[111]$  rod axis and the  $(\bar{1}01)$  plane. (a) Structure with cells and microbands. (b) Diffraction pattern of encircled area of Figure 4a.

band boundary is about  $2^\circ$ . The thickness of a microband is about 0.15 microns.

Another foil, whose plane was  $(\bar{1}\bar{1}2)$ , was also prepared parallel to the longitudinal section. Microbands

were observed not parallel to the drawing direction but to the  $[132]$  direction. The thickness of a microband was about 0.2 microns.

These results of the three foils show that each microband has a ribbon-like or plate-like form as was originally reported for silicon-iron.<sup>3,4</sup> The microbands lie in a matrix of equiaxed cells. The orientation of the microband is analyzed in Figure 5 using a  $(001)$  pro-

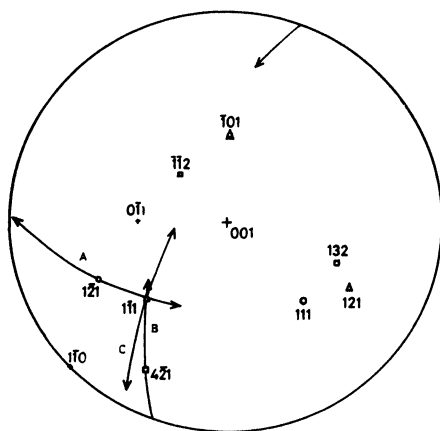


FIGURE 5.  $(001)$  standard projection for trace analysis. Circles correspond to the observations in the foil parallel to the cross section  $[(111)]$  while triangles and squares relate to the specimens cut parallel to the rod axis  $[(\bar{1}01)$  and  $(\bar{1}\bar{1}2)]$ . The lines parallel to great circles show an orientation spread of  $\pm 35^\circ$ .

jection. In the foil of the cross section with  $(111)$  parallel to the foil plane, the microbands extended parallel to the  $[\bar{1}01]$  direction. Therefore, the normal to the microband boundary must lie somewhere on the great circle named A. In the longitudinal foils parallel to  $(\bar{1}01)$  or  $(\bar{1}\bar{1}2)$ , the microbands extended parallel to  $[121]$  or  $[132]$ . Hence, the normal to the microbands must lie on the great circles B and C. Since the great circles A, B and C intersect at the pole of the  $(111)$  plane, the microband boundary is therefore parallel to  $(111)$  as already observed for rolled copper polycrystals of high purity.<sup>7</sup>

The thickness of the microbands and the sharpness of their boundaries differed from foil to foil. This can be explained on the basis of angular variations between the boundary plane and the foil plane. When the  $\{111\}$  plane, on which the boundary lies, makes a right

angle to the foil surface, the microband is imaged thinnest and its boundary is sharpest as shown in Figure 4. The misorientation across a microband boundary was in the range of 1 to 2° for almost all the cases observed. The boundary is therefore considered to be a small-angle boundary of the mixed type. Furthermore, it appears reasonable to assume that the lines of etch pits in the optical micrograph (Figure 2) corresponded at the intersections of the specimen plane with the large groups of microbands.

The results are summarized for the  $\langle 111 \rangle$  crystal as follows: (1) In a triangular area the orientation was almost unchanged. (2) In a matrix of equiaxed cells, groups of microbands developed parallel to  $\{111\}$  planes, i.e. microbands are not stretched out parallel to the drawing direction.

*The  $\langle 100 \rangle$  Crystal*

As in a former publication<sup>1</sup> some deformation bands were found in the core of the  $\langle 100 \rangle$  crystal drawn to 80%. The largest one was in the center of the rod and had an almost square cross section with a side length of 1.1 mm. Although it was microscopically recognized as a deformation band, its orientation had a large spread as shown by the  $\{111\}$  pole figure in Figure 6 and by the etch pits in the cross section in Figure 7. Besides etch pits with

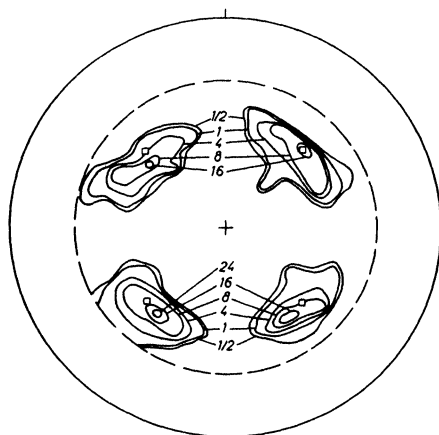


FIGURE 6.  $\{111\}$  pole figure of the cross section of the  $\langle 100 \rangle$  crystal. Intensities are in arbitrary units; squares indicate the ideal  $\langle 100 \rangle$  orientation.

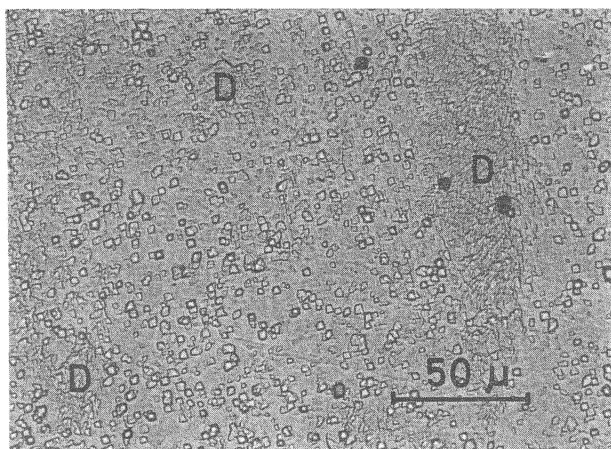


FIGURE 7. Etch figures in an optical micrograph of the cross section of the  $\langle 100 \rangle$  crystal. The sample is etched with solution (2). In regions D the orientation deviates from  $\langle 100 \rangle$ .

the square or nearly square form, those with irregular shapes were also observed, which indicate a deviation from the  $\langle 100 \rangle$  orientation (D in Figure 7). These regions are often very small (20 microns), and they make no clear boundary with the matrix. The hardness number of the cross section was much lower than in the  $\langle 111 \rangle$  crystal and had values between 98 and 105.

An electron micrograph in Figure 8a shows a typical structure of the  $\langle 100 \rangle$  deformation band. The foil was prepared almost parallel to the (011) plane in a longitudinal section. The density of dislocations is rather low as compared with that in  $\langle 111 \rangle$ . Cells are uniformly elongated in the [100] direction, i.e. in the drawing direction. They are about 0.35 microns in width. Figure 8b is a diffraction pattern from the encircled area in Figure 8a, showing that the misorientation across a cell boundary is very small. Because of the relative low density of dislocations, bending contours often appeared; and these made it difficult to resolve the cell structure in a wide range clearly.

In a foil prepared parallel to the cross section, a network of cells was observed (Figure 9a). The cells had a diameter of about 0.35 microns. The diffraction pattern in Figure 9b shows that (100) was in the foil plane and that the misorientation between adjoining cells was very small.

The above observation on two foils indicates that the cells have a cylindrical form, extending with their long axes parallel to the rod axis. The cell walls are

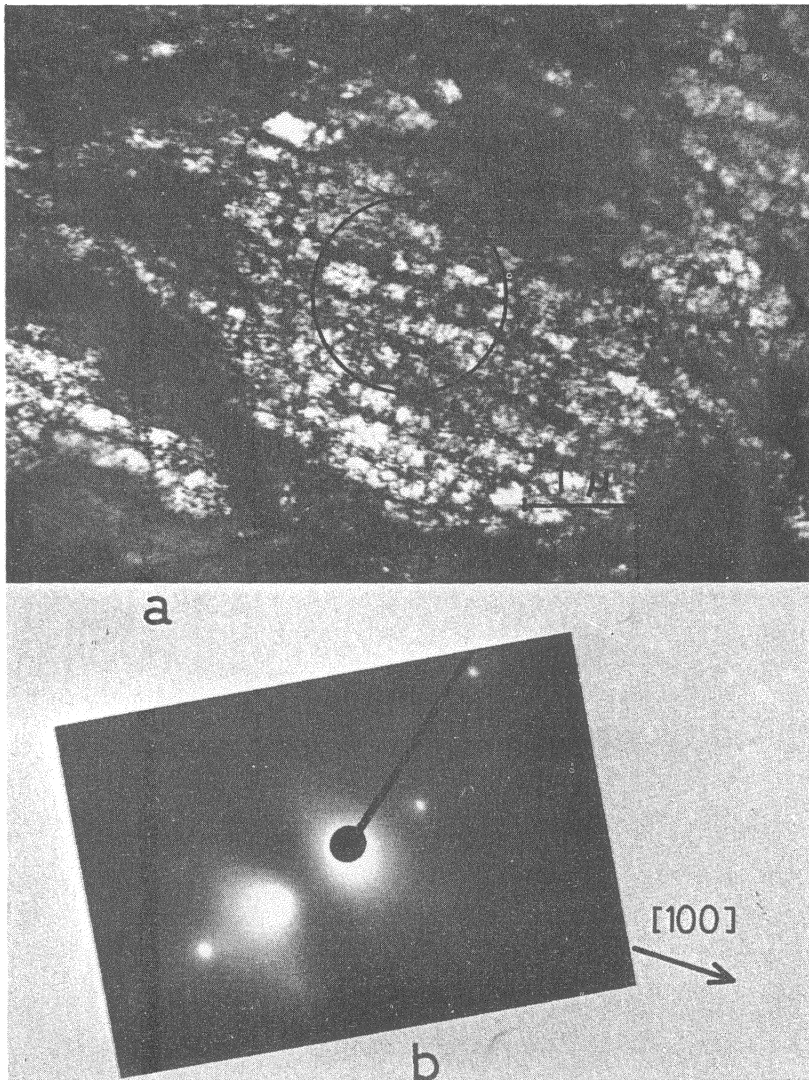


FIGURE 8a and b. Electron microscopic examination of a foil parallel to the  $[100]$  rod axis and the  $(011)$  plane. (a) Structure with cells elongated in the  $[100]$  direction. (b) Diffraction pattern of the encircled area in Figure 8a.

composed of a small number of dislocations, and this seems to be consistent with the low hardness observed.

Microbands were often observed among the cylindrical cells. Figure 10a shows microbands in the longitudinal

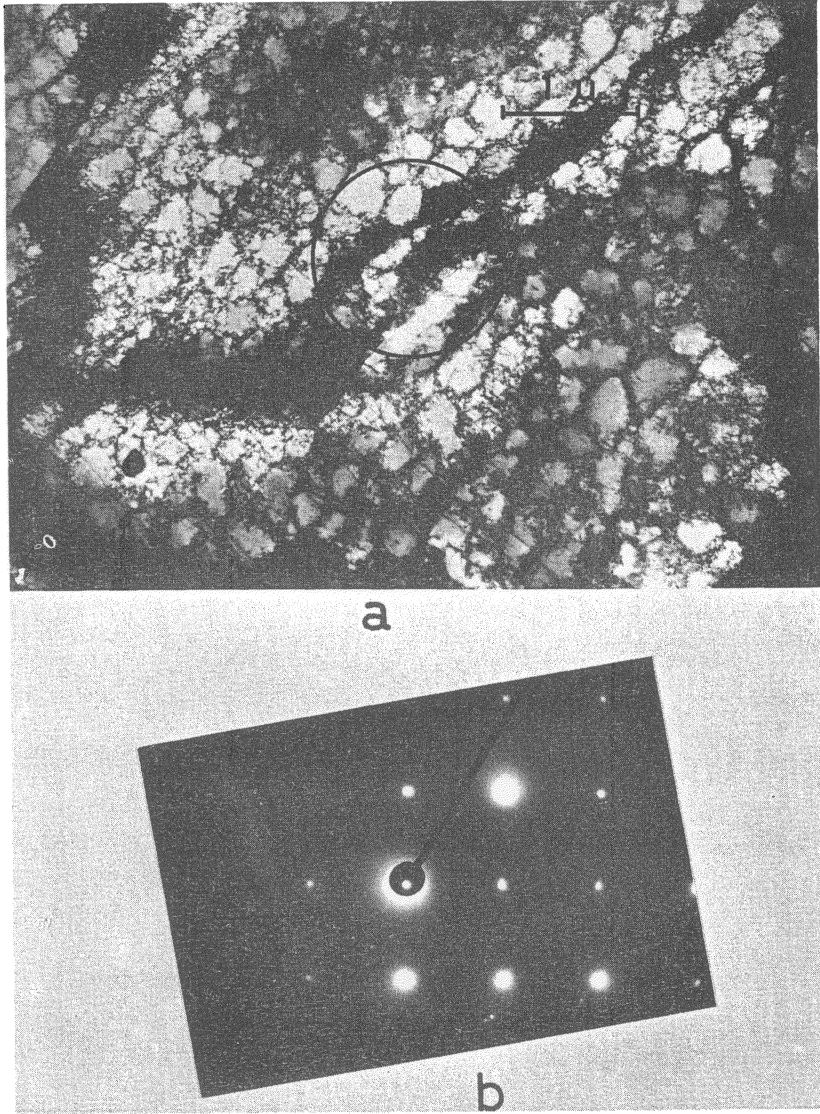


FIGURE 9a and b. (a) Cells in a specimen cut parallel to the cross section of the  $\langle 100 \rangle$  crystal. (b) Diffraction pattern of the encircled area in Figure 9a, showing that (100) is parallel to the foil plane.

foil cut parallel to the (011) plane. In most cases single microbands were observed, i.e. no groups of microbands developed. In the (011) foil the microbands were inclined  $30$  to  $35^\circ$  to the drawing direction suggesting

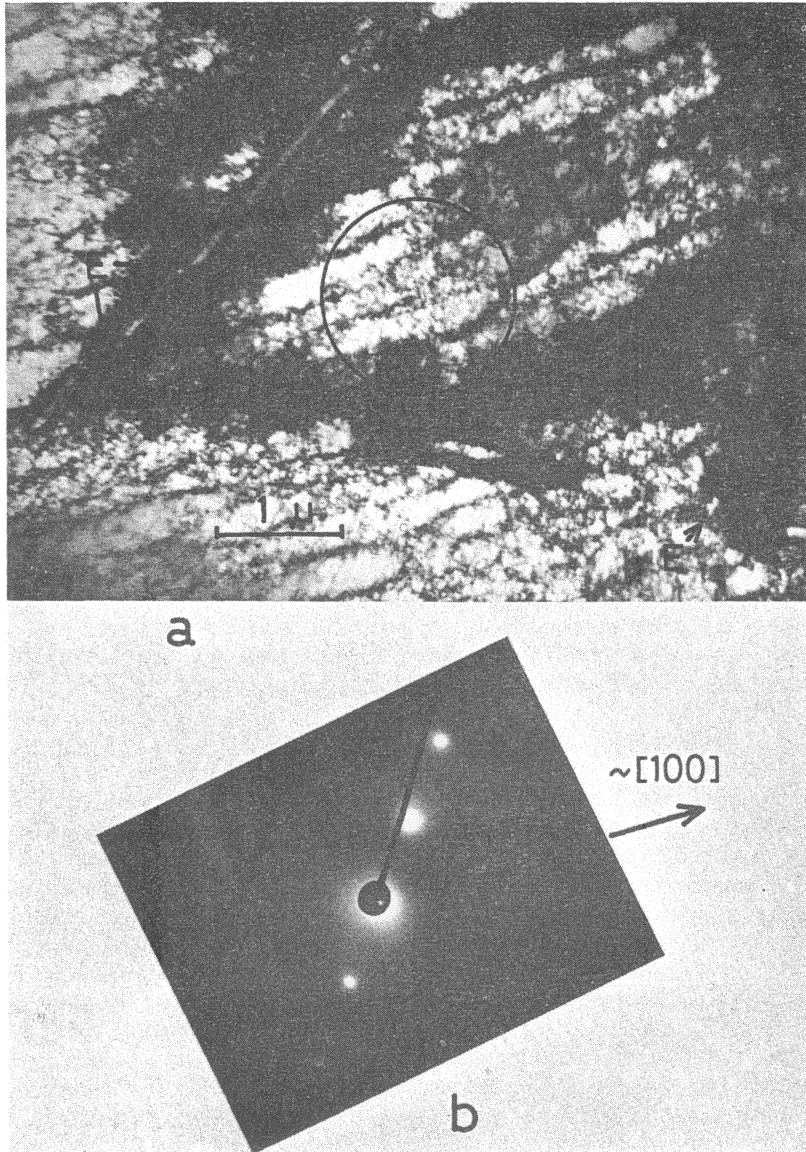


FIGURE 10a and b. (a) Structure in a longitudinal section of the  $\langle 100 \rangle$  crystal, which is almost parallel to the (011) plane. (b) Diffraction pattern of the encircled area in Figure 10a.

that they were almost parallel to the  $[2\bar{1}1]$  and  $[\bar{2}1\bar{1}]$  directions (Figure 10a and b). The microbands had sharp boundaries and their thickness was between 0.1 and 0.15 microns. It is to be noted that they are locally kinked

(parts E). As the diffraction spots in Figure 10b show, the spread of the orientation of the cells in the matrix was very small.

In a foil prepared parallel to the cross section, isolated microbands extended parallel to the  $\langle 011 \rangle$  directions of the cylindrical cells (F in Figure 11a). These microbands had no sharp boundaries and the reason for this is that not only the microbands were not perpendicular to the foil plane but also consisted of dislocation tangles. Figures 10 and 11 and their analysis show that the microbands lie parallel to  $\{111\}$  planes as in the  $\langle 111 \rangle$  crystal.

Figure 12a was taken about 15 microns away from the area shown in Figure 11. It shows that both structure and orientation changed abruptly. The dislocation tangles around the microbands were more dense in Figure 12a than in Figure 11a, and moreover, the network of cylindrical cells was no longer clearly observed. Large rectangular areas were formed with high dislocation density.

The diffraction spots in Figure 12b show some splitting but the orientation is still well within the spread of the pole figure, Figure 6. It can be assumed that the structure of Figure 12 belongs to areas like part D in Figure 7.

The observations made in foils of the  $\langle 100 \rangle$  crystal may be summarized as follows: (1) The core of the  $\langle 100 \rangle$  crystal showed larger orientation spread than that of the  $\langle 111 \rangle$  crystal. (2) In this area of a deformation band cylindrical cells were formed. The long axes of the cells were parallel to  $\langle 100 \rangle$ , i.e. to the drawing direction. (3) In local regions of the deformation band deviation from  $\langle 100 \rangle$  occurred. (4) This orientation change is apparently connected with the development of microbands which cause the destruction of the cylindrical cells. (5) As in the case of the  $\langle 111 \rangle$  crystal, the boundaries of the microbands lie on  $\{111\}$  planes. (6) Tangling of dislocations occurred around the microbands and large rectangular areas were formed alternately.

## DISCUSSION

As already shown<sup>2-4</sup>, the orientation is changed as a result of the formation of microbands. This process can be seen especially clearly in the  $\langle 100 \rangle$  crystal. In the  $\langle 100 \rangle$  deformation band cylindrical cells are often crossed with isolated microbands. Dislocation tangles around them then occur and destroy the cell structure.

In the  $\langle 111 \rangle$  crystal, groups of microbands are formed and only the orientation spread increased in the course of deformation. The lattice rotations at each

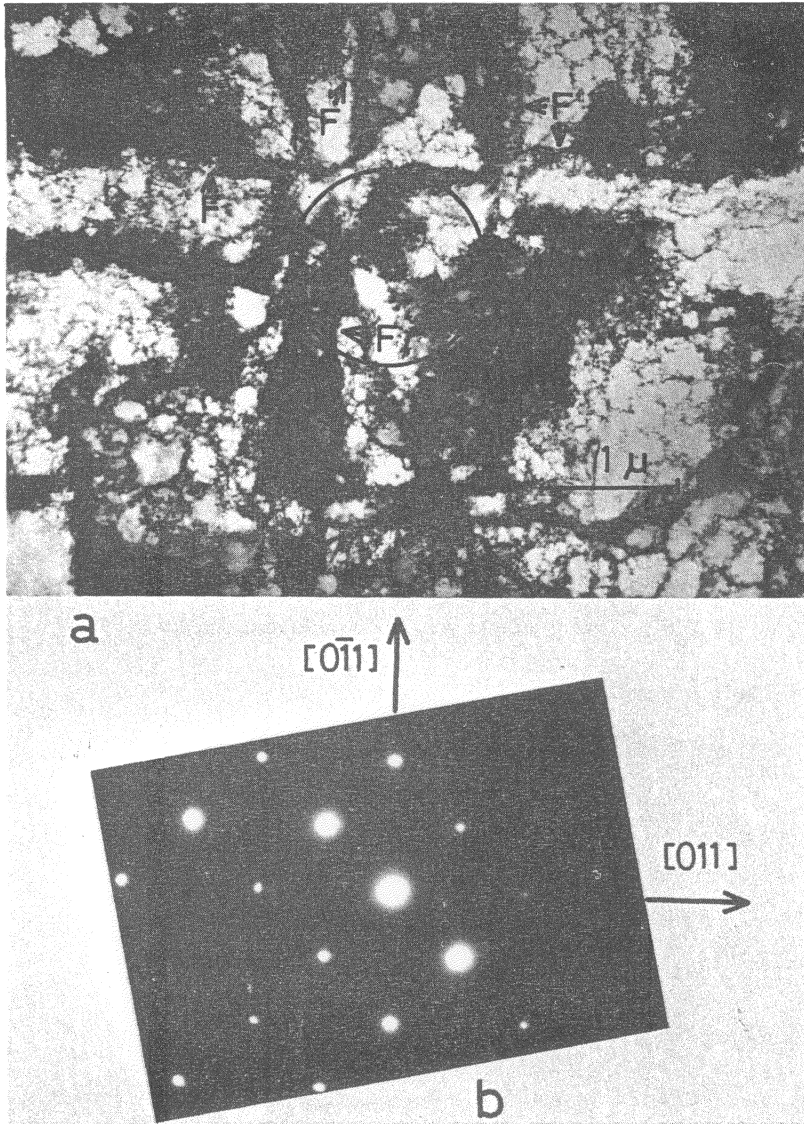


FIGURE 11a and b. (a) Structure in a foil prepared parallel to the cross section  $[(100)$  plane] of the  $\langle 100 \rangle$  crystal. In areas F isolated microbands parallel to  $\langle 011 \rangle$  directions can be seen. (b) Diffraction pattern of the encircled area in Figure 11a.

group of microbands often occur in opposite directions (Figure 3). The total orientation spread does not become very large.

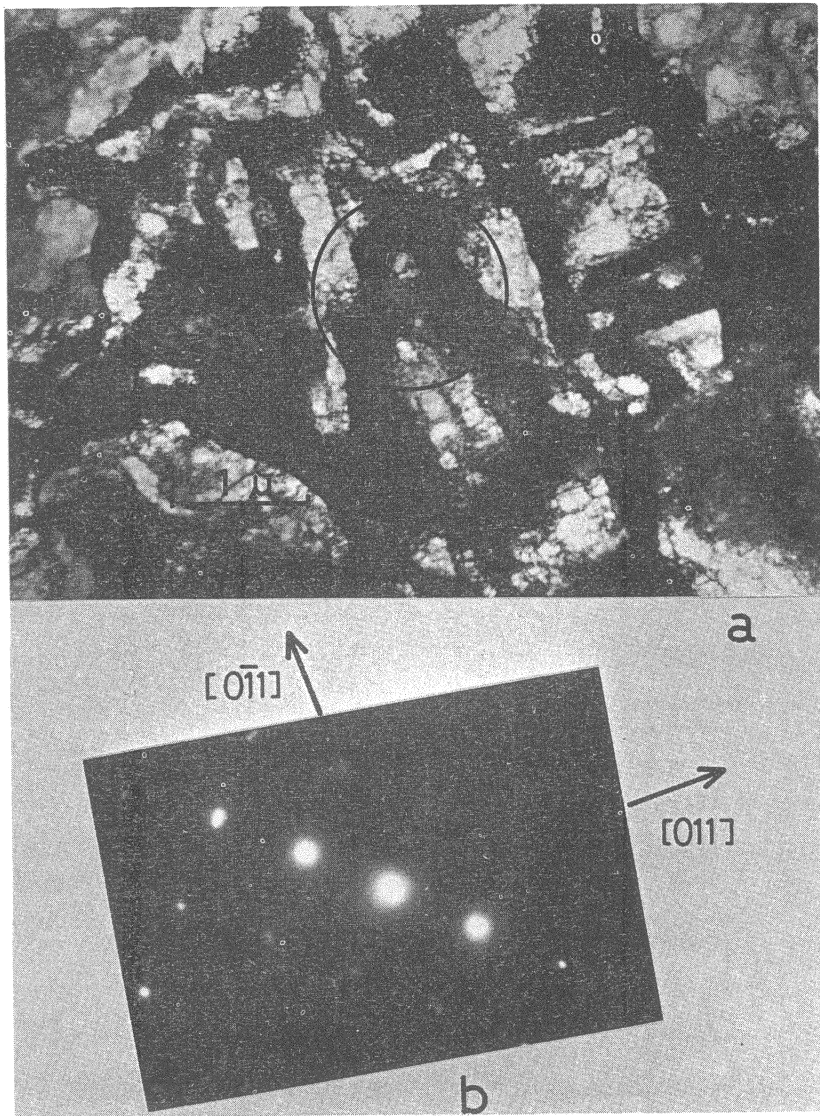


FIGURE 12a and b. (a) Structure in the same foil as used in Figure 11 but about 15 microns away from it. (b) Diffraction pattern of the encircled area in Figure 12a.

This study shows, at least for the  $\langle 100 \rangle$  starting orientation, that the microbands were formed independent of the cells existing in the matrix. This is supported especially by the different morphology of cylindrical cells extending parallel to  $\langle 100 \rangle$  and of microbands

lying parallel to  $\{111\}$ . Microbands are developed as such, and are not further derived from the cells. Such an interpretation is also supported by the studies of copper single crystals deformed by plane-strain deformation.<sup>8</sup> In spite of these observations the exact mechanism of microband formation is still not known.

It was reported that microbands in copper single crystals<sup>11</sup> and polycrystals<sup>9,10</sup> extended parallel to the drawing direction after reduction of more than 95%. This is considered to be a result of the orientational changes of the microband boundaries by slip at higher degrees of reduction, although they were originally formed parallel to  $\{111\}$  planes. Microbands, whose boundaries deviated from  $\{111\}$  planes and tended to become parallel to the drawing direction, were also found in this study (Figure 10).

It has been shown by various authors<sup>12-15</sup> that the  $\langle 100 \rangle$  annealing texture can be developed by strain-induced grain boundary migration of the  $\langle 100 \rangle$  component of the deformation texture. This observation was explained by the lower hardness and stronger tendency for recovery of the  $\langle 100 \rangle$  orientation. The basic reason for these phenomena must lie in the special dislocation structure of the orientation, such as those described in this work.

#### ACKNOWLEDGMENT

The authors wish to express their deep gratitude to Dipl.-Engs. T. Noda and J. Huber for their valuable discussion. A part of this study was done during the stay of one of the authors (S.H.) at the Technische Universität Clausthal as a scholar of the Alexander von Humboldt-Foundation.

#### REFERENCES

1. H. Ahlborn, *Z. Metallkunde*, 56, 411 (1965).
2. H. Ahlborn and D. Sauer, *Z. Metallkunde*, 59, 658 (1968).
3. J. L. Walter and G. F. Koch, *Acta Met.*, 11, 923 (1963).
4. H. Hu, in *Recovery and Recrystallization of Metals*, L. Himmel, ed., Interscience Publishers, New York, 1963, p. 311.
5. H. Ahlborn, in *Recrystallization, Grain Growth and Textures*, H. Margdin, ed., American Society for Metals, 1966, p. 374.
6. C. S. Barrett and T. B. Masalski, *Structure of Metals*, McGraw-Hill Book Co., New York, 1966, p. 551.
7. F. Bourelier and J. L. Hericy, 7th Coll. de métallurgie Saclay 1963, Press universitaires de France, p. 33.

8. J. Huber, unpublished results, and J. Erdmann, Diplomarbeit, Institut für Metallkunde TU Clausthal, 1974.
9. G. Mima, Y. Ogino, and J. Sato, *J. Inst. Met.*, 96, 49 (1968).
10. J. H. Clairns, J. Clough, M. A. P. Dewey, and J. Nutting, *J. Inst. Met.*, 99, 93 (1971).
11. D. Sauer, Diplomarbeit, Institut für Metallkunde TU Clausthal, 1968.
12. R. A. Vandermeer and C. J. McHargue, *Trans. AIME*, 230, 667 (1964).
13. H. Ahlborn, G. Wassermann and S. Wiesner-Kaup, *Z. Metallkunde*, 57, 22 (1966).
14. J. Grewen, *Z. Metallkunde*, 57, 581 (1966).
15. T. Noda, Doktorarbeit, Institut für Metallkunde TU Clausthal, 1974.